

# Cold Fronts from Shock Collisions

Yuval Birnboim<sup>1</sup>, Uri Keshet<sup>1\*</sup> & Lars Hernquist<sup>1</sup>

<sup>1</sup>*Harvard-Smithsonian Center for Astrophysics, 60 Garden Street, Cambridge MA, USA*

Accepted —. Received —; in original —

## ABSTRACT

Cold fronts (CFs) are found in most galaxy clusters, as well as in some galaxies and groups of galaxies. We propose that some CFs are relics of collisions between trailing shocks. Such a collision typically results in a spherical, factor  $\approx 1.4 - 2.7$  density/temperature discontinuity. These CFs may be found as far out as the virial shock, unlike what is expected in other CF formation models.

As a demonstration of this effect, we use one dimensional simulations where halo reverberations involving periodic collisions between the virial shock and outgoing secondary shocks exist. These collisions yield a distinctive, concentric geometric sequence of CFs which trace the expansion of the virial shock.

**Key words:** galaxies: clusters: general – galaxies: haloes – X-rays: galaxies: clusters – shock waves

## 1 INTRODUCTION

Recent X-ray observations of galaxy clusters reveal various phenomena in the gaseous haloes of clusters, such as mergers, cavities, shocks and cold fronts (CFs). CFs are thought to be contact discontinuities, where the density and temperature jump, while the pressure remains continuous (up to projection/resolution effects). They are common in clusters (Markevitch & Vikhlinin 2007) and vary in morphology (they are often arcs but some radial or filamentary CFs exist), contrast (the density jump is scattered around a value of  $\sim 2$ ), quiescence (some are in highly disturbed merging regions, and some in smooth, quiet locations), and orientation. CFs have been postulated to originate from cold material stripped during mergers (Markevitch et al. 2000, for example) or sloshing of the intergalactic medium (IGM; Markevitch et al. 2001; Ascasibar & Markevitch 2006). In some cases, a metallicity gradient is observed across the CF, indicating that it results from stripped gas, or radial motions of gas (see Markevitch & Vikhlinin 2007, and references therein). Shear is often found along CFs in relaxed clusters, implying nearly sonic bulk flow beneath the CF (Keshet et al. 2009). Whether CFs are present at very large radii ( $\gtrsim 500$  kpc) is currently unknown because of observational limitations.

In what follows, we propose that some CFs are produced by collisions between shocks. When two trailing shocks collide, a CF is always expected to form. Its parameters can be calculated by solving the shock conditions and corresponding Riemann problem. Most of the scenarios in which

shocks are produced (quasars, AGN jets, mergers) predict that shocks will be created at, or near, a cluster center, and expand outwards (albeit not necessarily isotropically). When one shock trails another, it always propagates faster (supersonically with respect to the subsonic downstream flow of the leading shock), so collisions between outgoing shocks in a cluster are inevitable if they are generated within a sufficiently short time interval.

In § 2 we solve for the parameters of CFs that are caused by a collision between two arbitrary planar shocks. As a demonstration of the general mechanism, we show in § 3, using 1D spherical cluster simulation that collisions between the virial shock and a secondary shock are expected to produce a distinct pattern of CFs. In § 4 we compare the features of observed CFs with results from our analysis, and list some model-specific predictions. In § 5 we summarize and conclude.

## 2 COLLISION BETWEEN TWO TRAILING SHOCKS

In this section we examine two planar shocks moving in the same direction and calculate the contact discontinuity that forms when the second shock overtakes the leading one. This problem is fully characterized (up to normalization) by the Mach numbers of the first and second shocks,  $M_0$  and  $M_1$ . At the instant of collision, a discontinuity in velocity, density and pressure develops, corresponding to a Riemann problem (second case in Landau & Lifshitz 1959, §93). The discontinuity evolves into a (stronger) shock propagating in the initial direction and a reflected rarefaction wave, sepa-

\* Einstein fellow

rated by a contact discontinuity which we shall refer to as a shock induced CF (SICF). The density is higher (and the entropy lower) on the SICF side closer to the origin of the shocks. This yields a Rayleigh-Taylor stable configuration if the shocks are expanding outwards. Now, we derive the discontinuity parameters.

### 2.1 The discontinuity contrast

We consider an ideal gas with an adiabatic constant  $\gamma$ . Before the shocks collide, denote the unshocked region as zone 0, the region between the two shocks as zone 1, and the doubly shocked region as zone 2. After the collision, regions 0 and 2 remain intact, but zone 1 vanishes and is replaced by two regions, zone  $3_o$  (adjacent to zone 0; the outer region for outgoing spherical shocks) and zone  $3_i$  (adjacent to 2; inner), separated by the SICF. We refer to the plasma density, pressure, velocity and speed of sound respectively as  $\rho$ ,  $p$ ,  $u$  and  $c$ . Velocities of shocks at the boundaries between zones are denoted by  $v_i$ , with  $i$  the upstream zone. We rescale all parameters by the unshocked parameters  $\rho_0$  and  $p_0$ .

The velocity of the leading shock is

$$v_0 = u_0 + M_0 c_0, \quad (1)$$

where

$$c_i = \left( \frac{\gamma p_i}{\rho_i} \right)^{1/2} \quad (2)$$

for each zone  $i$ . Without loss of generality, we measure velocities with respect to zone 0, implying  $u_0 = 0$ .

The state of zone 1 is related to zone 0 by the Rankine-Hugoniot conditions,

$$p_1 = p_0 \frac{2\gamma M_0^2 - \gamma + 1}{\gamma + 1}, \quad (3)$$

$$u_1 = u_0 + \frac{p_1 - p_0}{\rho_0(v_0 - u_0)}, \quad (4)$$

$$\rho_1 = \rho_0 \frac{u_0 - v_0}{u_1 - v_0}. \quad (5)$$

The state of the doubly shocked region (zone 2) is related to zone 1 by reapplying equations 1- 5 with the subscripts 0, 1 replaced respectively by 1, 2, and  $M_0$  replaced by  $M_1$ .

Across the contact discontinuity that forms as the shocks collide (the SICF), the pressure and velocity are continuous but the density, temperature and entropy are not; the CF contrast is defined as  $q \equiv \rho_{3_i}/\rho_{3_o}$ . Regions 0 and  $3_o$  are related by the Rankine-Hugoniot jump conditions across the newly formed shock,

$$p_3 = p_0 \frac{(\gamma + 1)\rho_{3_o} - (\gamma - 1)\rho_0}{(\gamma + 1)\rho_0 - (\gamma - 1)\rho_{3_o}}, \quad (6)$$

$$u_3 - u_0 = \left[ (p_3 - p_0) \left( \frac{1}{\rho_0} - \frac{1}{\rho_{3_o}} \right) \right]^{1/2}. \quad (7)$$

The adiabatic rarefaction from pressure  $p_2$  down to  $p_3 = p_{3_i} = p_{3_o}$  is determined by

$$u_2 - u_3 = -\frac{2c_2}{\gamma - 1} \left[ 1 - \left( \frac{p_3}{p_2} \right)^{(\gamma-1)/2\gamma} \right]. \quad (8)$$

The system can be solved by noting that the sum of eqs. (7) and (8) equals  $u_2 - u_0$ , fixing  $\rho_{3_o}$  as all other parameters are known from eqs. (1-6).

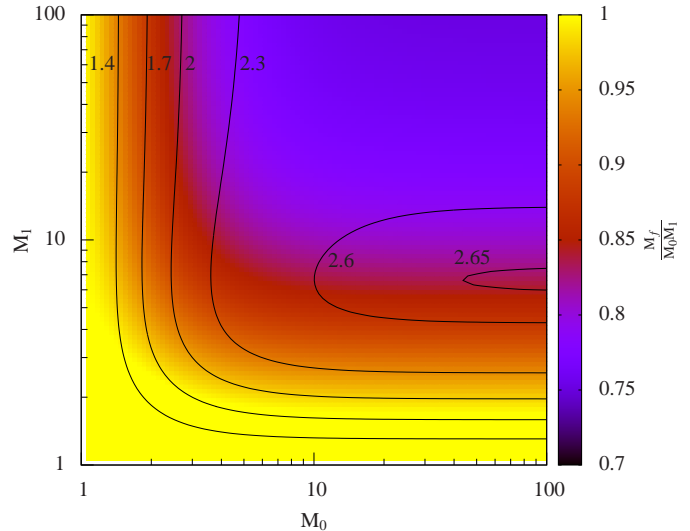


**Figure 1.** Contrast  $q$  of a CF generated by a collision between two trailing shocks with Mach numbers  $M_0$  and  $M_1$ , for  $\gamma = 5/3$  (labeled contours). The color map shows the final Mach number  $M_f$  normalized by  $M_0 M_1$ .

Finally, the Mach number of the new shock and the rarefacted density are given by

$$M_f^2 = \frac{2\rho_{3_o}/\rho_0}{(\gamma + 1) - (\gamma - 1)\rho_{3_o}/\rho_0}, \quad (9)$$

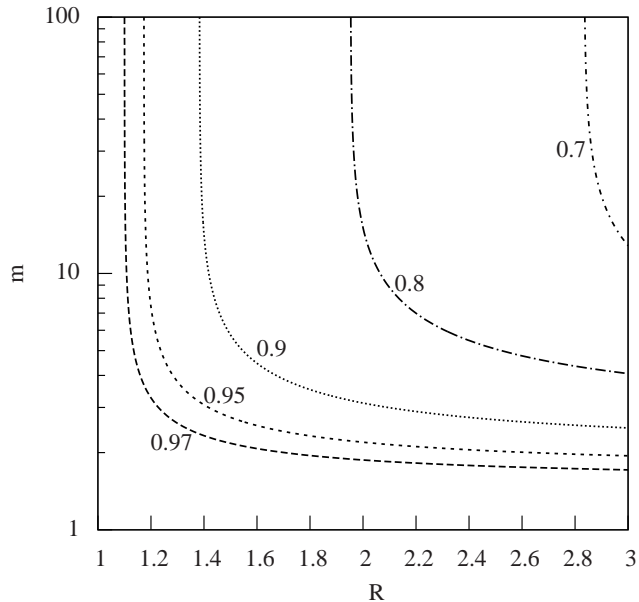
$$\rho_{3_i} = \rho_2 (p_3/p_2)^{1/\gamma}. \quad (10)$$

Figure 1 shows the discontinuity contrast  $q$  for various values of  $M_0$  and  $M_1$ , for  $\gamma = 5/3$ . Typically  $q \sim 2$ , ranging from 1.45 for two Mach 2 shocks, for example, to  $q_{max}$ . The maximal contrast  $q_{max}$  depends only on the adiabatic index; for  $\gamma = 5/3$  we find  $q_{max} = 2.653$ , achieved for  $M_0 \gg 1$  and  $M_1 \simeq 6.65$ . The possible contrast range of SICFs is in good agreement with the CF contrasts observed (Markevitch & Vikhlinin 2007; Owers et al. 2009). The figure colorscale shows the dimensionless factor  $f$  defined by  $M_f = fM_0M_1$ , ranging between 0.75 and 1 for  $1 < \{M_0, M_1\} < 100$ .

### 2.2 Stability of Shock Induced Cold Fronts

The stability of CFs limits the time duration over which they are detectable, and so is important when comparing CF formation models with observations. Various processes can cause a gradual breakup or smearing of the CF. They act in CFs regardless of their formation mechanism.

Thermal conduction and diffusion of particles across the CF smears the discontinuity on a timescale that is set by the thermal velocity and the mean free path of the protons. The Spitzer m.f.p.  $\lambda$  in an unmagnetized plasma with typical cluster densities is a few kpc, and depends on the thermal conditions on both sides of the discontinuity (Markevitch & Vikhlinin 2007). Taking  $\lambda \sim 10$  kpc and a thermal velocity  $\bar{v} \sim 1000$  km sec $^{-1}$ , and assuming that a CF is visible if it is sharper than  $L_{obs} \sim 10$  kpc, we get a characteristic timescale for CF dissipation,



**Figure 2.** Fractional decline (contours) in initial CF contrast  $q$  induced by a collision with a shock of Mach number  $m$  arriving from the dense CF side, for  $\gamma = 5/3$ . The vertical dashed line corresponds to the maximal SICF contrast,  $q_{max}$ .

$$t \sim \frac{L_{obs}^2}{D} \sim \frac{3L_{obs}^2}{\bar{v}\lambda} \sim 10^7 \text{ yr.} \quad (11)$$

This result indicates that in order for shock induced CFs to be observable, either (i) they are formed frequently (e.g., by a series of AGN bursts; see Ciotti & Ostriker 2007; Ciotti et al. 2009); or (ii) magnetic fields reduce the m.f.p. considerably, as some evidence suggests (see the discussion in Lazarian 2006).

Note that the heat flux driven buoyancy instability (HBI) tends to preferentially align magnetic fields perpendicular to the heat flow in regions where the temperature decreases in the direction of gravity. This effect could reduce radial diffusion within the inward cooling regions in the cores of cool core clusters (Quataert 2008; Parrish et al. 2009). Across a CF transition there is a sharp temperature drop towards the inner side, in the direction of gravity. Heat flow could induce HBI on the scale width of the CF, aligning the magnetic fields parallel to the discontinuity and diminishing radial diffusion. This possibility needs to be addressed further by detailed numerical magneto-hydrodynamic simulations.

CFs could be degraded by subsequent shocks that sweep outwards across the CF. However, the CF contrast is only slightly diminished by this effect, by  $< 4\%$  for  $q < 2$  and a shock Mach number  $m < 2$ , as shown in fig. 2. Such passing shocks seed Richtmyer-Meshkov instabilities which could cause the CF to break down. Although less efficient than Rayleigh-Taylor instabilities, these instabilities operate regardless of the alignment with gravity. The outcome depends on  $m$  and on any initial small perturbations in the CF surface. However, the instability is suppressed if the CF becomes sufficiently smoothed.

It is worth noting that KHI, which could break down CFs formed through ram pressure stripping and sloshing,

does not play an important role in SICFs because there is little or no shear velocity across them. On the other hand, the stabilizing alignment of magnetic fields caused by such shear (Markevitch & Vikhlinin 2007) is also not expected here.

### 3 A CLUSTER SCALE REVERBERATION MODE

At the edge of galaxy clusters there are virial shocks with typical Mach numbers  $\sim 30 - 100$ , heating the gas from  $\sim 10^4$  K to  $\sim 10^7$  K by converting kinetic energy into thermal energy. The rate of expansion of a virial shock is set on average by the mass flux and velocity of the infalling material (see for example Bertschinger 1985). We find in our simulations that while this expansion is steady on average, the shock sometimes oscillates, moving faster or slower than the steady state expansion. This creates periods dominated by alternating halo compression and expansion. During periods of enhanced compression in the outer halo regions, when the shock slows down, compression is sent inwards and is reflected through the center, gradually steepening into an outgoing shock. When this shock collides with the virial shock, a situation corresponding to that described in § 2, bouncing the virial shock into another cycle of reverberation, creating an SICF and sending inwards a steep rarefaction<sup>1</sup>. This rarefaction marks the end of the compression period of the next cycle setting the oscillation period to approximately the sound crossing time, in and out across the cluster. The combined effect is a long-lived, coherent “breathing” mode. Such “breathing” oscillations are observed in the 3D galactic and cluster halo simulations of Kereš & Hernquist (2009)<sup>2</sup>.

Using 1D spherical simulations of the formation of clusters from initial cosmic perturbations (Birnboim & Dekel 2003), we test the formation and evolution of associated SICFs. The simulation includes baryonic shells, dark matter shells, and angular momentum support. The oscillatory mode in the simulation has not been intentionally excited, and results from stochastic inner core ( $\sim 0.05R_{vir}$ ) vibrations as external dark matter shells with low angular momentum interact gravitationally with the core. Physically, any waves, shocks or gravitational perturbations (mergers or AGNs) will contribute to the mode, as well as non-smooth accretion rates that would cause the virial shock to vibrate. A more detailed examination of this is beyond the scope of this letter (note, however, that the strength of the SICF depends only weakly on the parameters of the secondary shock and is always close to 2.)

Fig. 3 shows the evolution of a  $3 \times 10^{14} M_{\odot}$  halo until redshift  $z = 0$  (an adiabatic version of those described in Birnboim & Dekel 2009, *in prep.*). The expanding virial shock is traced by a jump in the velocity of the Lagrangian shells (red, thin lines), and by the shock-finding algorithm that is based on entropy increase along Lagrangian shells (blue region). The outgoing, secondary shocks that reach the virial shock periodically are also clearly visible. The virial shock bounces outwards each time it is hit by a secondary. A

<sup>1</sup> A movie of the evolution of radial profiles in time is available at <http://www.cfa.harvard.edu/~ybirnboi/SICF/sicf.html>

<sup>2</sup> Dušan Kereš, (private communication).

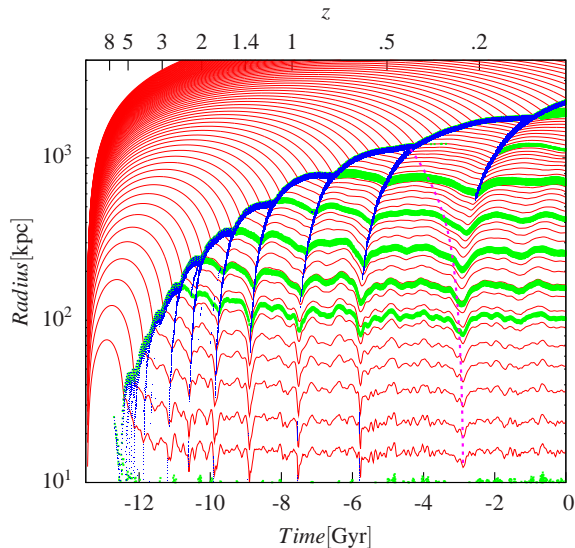


**Figure 3.** Evolution of a galaxy cluster from cosmological initial perturbations. The final mass of the cluster at  $z = 0$  is  $3 \times 10^{14} M_{\odot}$ . The radius and time of Lagrangian shells (every 25<sup>th</sup> shell) are plotted in red thin lines. Shocks are traced by large Lagrangian derivatives of the entropy ( $d \ln S / dt > .1 \text{ Gyr}^{-1}$ , blue dots), and CFs are traced by their large entropy gradients ( $\partial \ln S / \partial \ln r > 0.5$ , green dots). Rarefaction waves can be seen as small motions of the Lagrangian shells (illustrated by the dashed magenta curve, manually added based on a time series analysis). Their trajectory is approximately the reflection of the preceding outgoing compression, time inverted about the last secondary-virial shock collision.

rarefaction wave is reflected inwards (illustrated by a dashed curve), and a spherical SICF is left behind. The SICFs are visible through the entropy gradients (green region), and, in the absence of diffusion and instabilities, persist until  $z = 0$ . As expected, the interaction of the discontinuity with subsequent shocks (§2.2; fig. 2) does not considerably reduce the CF contrast. Fig. 4 shows the entropy, pressure, density and temperature profiles of this simulation at  $z = 0$ . A series of SICFs (marked with blue vertical lines) is visible, seen as entropy jumps with continuous pressure. The density jumps by roughly a factor of  $q \sim 2$ , as expected, with the temperature dropping accordingly.

The SICFs formed in this simulation are almost static, and roughly logarithmically spaced. The calculations presented in Figures 3-4 are adiabatic. When cooling is turned on in the absence of feedback, this simulation suffers from overcooling, creating an overmassive BCG of  $2 \times 10^{12} M_{\odot}$  and star formation rates of  $100 M_{\odot} \text{ yr}^{-1}$ , and the luminosity exceeds the  $L_x - T$  relation. The excitation of the basic mode, and periodic CFs, are observed in all these simulations. The simulation presented here was performed with 2,000 baryonic and 10,000 dark matter shells. When the resolution is lowered to 250 baryonic shells, the reverberation amplitude and periods are essentially unchanged, indicating that the results are well converged.

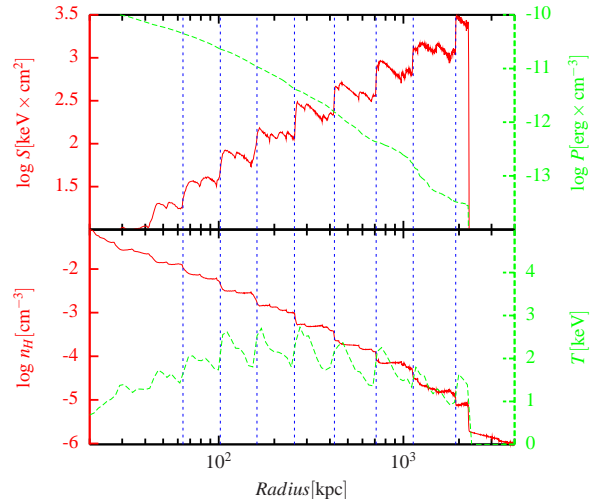


**Figure 4.** Thermodynamic profile of the simulated cluster shown in Fig. (3) at  $z = 0$ . *Top:* entropy (red, solid, left axis) and pressure (green, dashed, right axis). *Bottom:* density (red, solid, left axis) and temperature (green, dashed, right axis). CFs are marked with blue dashed vertical lines.

#### 4 OBSERVABILITY OF SHOCK INDUCED COLD FRONTS

Owers et al. (2009) present high quality Chandra observations of 3 relaxed CFs. They all seem concentric with respect to the cluster center, and spherical in appearance. Owers et al. (2009) interpret these as evidence for sloshing, and find spiral characteristics in 2 of them. We argue here that some CFs of this type could originate from shock collisions. In the SICF model, CFs are spherical, unlike the truncated CFs formed by ram pressure stripping or sloshing, so no special projection orientation is required. On the other hand, SICFs do not involve metallicity discontinuities, observed in some of these CFs. The observed contrasts of these CFs are quite uniform, with best fit values in the range 2.0 – 2.1 (with  $\sim 20\%$  uncertainty) in all three, as expected for SICFs<sup>3</sup>.

The SICF formation model is entirely distinct from ram pressure stripping and sloshing CFs, and it makes many different predictions.

**Morphology.** SICFs are quasi-spherical around the source of the shocks. A galactic merger defines an orbit plane, and the corresponding perturbation (stripped material or center displacement) will create CFs parallel to this plane. In some sloshing scenarios (Ascasibar & Markevitch 2006) the CFs extend considerably above the plane, but would never appear as a full circle on the sky; an observed CF “ring” would strongly point towards an SICF. The statistical properties of a large CF sample could thus be used to distinguish between the different scenarios.

**Amplitude.** SICFs have distinct entropy and density contrasts that depend weakly on shock parameters;  $q$  is typ-

<sup>3</sup> Note that collisions with outgoing shocks could diminish the contrast towards  $q \sim 2$ , regardless of CF origin. A larger, more complete sample of CFs is needed to determine the origin/s of the relaxed population.

ically larger than  $\sim 1.4$  (assuming  $M_1 \geq 2$ ) and is always smaller than  $q_{max} = 2.65$ .

**Extent.** If the cluster reverberation mode is excited, SICF radii should be approximately logarithmically spaced. Any shock that expands and collides with the virial shock will create SICF at the location of the virial shock, far beyond the core. The external SICFs are younger, and would appear sharper owing to less diffusion and collisions with secondary shocks. Deep observations capable of detecting CFs at  $r \sim 1$  Mpc are predicted to find SICFs (fig. 4). Such distant CFs occur naturally only in the SICF model.

**Plasma diagnostics.** Shocks are known to modify plasma properties in a non-linear manner, for example by accelerating particles to high energies and amplifying/generating magnetic fields. The plasmas on each side of an SICF may thus differ, being processed either by two shocks or by one, stronger shock. This may allow indirect detection of the CF, in particular if the two shocks were strong before the collision. For example, enhanced magnetic fields below the CF may be observable as excess synchrotron emission from radio relics that extend across the CF, in nearby clusters, using future high-resolution radio telescopes (LOFAR, SKA).

## 5 SUMMARY AND DISCUSSION

Our study consists of two parts. The first is a general discussion about CFs that form as a result of a collision between two trailing shocks. The second part describes a specific reverberation mode of galaxy and cluster haloes that has been identified in 1D simulations, and also seen in 3D. One aspect of these reverberations is periodic collisions between the virial shock and outgoing secondary shocks, resulting in SICFs – a special case of the mechanism discussed in the first part of our paper.

We have shown that when shocks move in the same direction they collide and generate a CF. The density contrast across the CF is calculated as a function of the Mach numbers of the two shocks. It is typically larger than 1.4 (if  $M \gtrsim 2$ ), and is always smaller than  $q_{max} = 2.65$ . The discontinuity is smeared over time by diffusion, at a rate that depends on the unknown nature and amplitude of magnetic fields. CFs are susceptible to heat-flux-driven buoyancy instability (HBI), which could align the magnetic field tangent to the CF and potentially moderate further diffusion. SICFs, like all other CFs, are subject to Richtmyer-Meshkov instabilities from subsequent shocks passing through the cluster. Such collisions reduce the CF contrast until it reaches  $q \sim 2$ . Unlike most other CF models, an SICF is not expected to suffer from KHI.

In § 3, using a 1D spherical hydrodynamic code to evolve cosmological perturbations, we demonstrate that a reverberation mode exists in the haloes of galaxies and clusters and causes periodic collisions between the virial shocks and secondary shocks that produce SICF. The simulated SICF contrast is consistent with the theoretical predictions of § 2. A more thorough investigation of this potentially important mode, including its stability in 3D is left for future works. We use it here as a specific scenario for SICF formation.

The predicted properties of SICFs are presented in

§4, and reproduce some of the CF features discussed in Owers et al. (2009). In particular, we suggest that CFs in relaxed clusters, with no evidence of mergers, shear, or chemical discontinuities, may have formed by shock collisions. We list the properties of SICFs that could distinguish them from CFs formed by other mechanisms. The SICF model predicts quasi-spherical CFs which are concentric about the cluster center, with contrast  $q \sim 2$ , and possibly extending as far out as the virial shock. An observed closed (circular/oval) CF could only be an SICF. In the specific case of cluster reverberation, a distinct spacing pattern between CFs is expected. It may be possible to detect them indirectly, for example as discontinuities superimposed on peripheral radio emission.

Shocks originating from the cluster center naturally occur in feedback models that are invoked to solve the overcooling problem. They are also formed by mergers of substructures with the BCG. Thus, SICFs should be a natural phenomenon in clusters. Further work is needed to assess how common SICFs are with respect to other types of CFs, and to characterize inner SICFs that could result, for example, from collisions between offset AGN shocks. The properties of reverberation in 3D will be pursued in future work.

## ACKNOWLEDGEMENTS

We thank M. Markevitch for useful discussions. YB acknowledges the support of an ITC fellowship from the Harvard College Observatory. UK acknowledges support by NASA through Einstein Postdoctoral Fellowship grant number PF8-90059 awarded by the Chandra X-ray Center, which is operated by the Smithsonian Astrophysical Observatory for NASA under contract NAS8-03060.

## REFERENCES

- Ascasibar Y., Markevitch M., 2006, ApJ, 650, 102
- Bertschinger E., 1985, ApJS, 58, 39
- Birnboim Y., Dekel A., 2003, MNRAS, 345, 349
- Ciotti L., Ostriker J. P., 2007, ApJ, 665, 1038
- Ciotti L., Ostriker J. P., Proga D., 2009, ApJ, 699, 89
- Kereš D., Hernquist L., 2009, ApJ, 700, L1
- Keshet U., Markevitch M., Birnboim Y., Loeb A., 2009, ArXiv e-prints
- Landau L. D., Lifshitz E. M., 1959, *Fluide Mechanics*. Pergamon press, 1959
- Lazarian A., 2006, ApJ, 645, L25
- Markevitch M., Ponman T. J., et al. 2000, ApJ, 541, 542
- Markevitch M., Vikhlinin A., 2007, Phys. Rep., 443, 1
- Markevitch M., Vikhlinin A., Mazzotta P., 2001, ApJ, 562, L153
- Owers M. S., Nulsen P. E. J., Couch W. J., Markevitch M., 2009, ApJ, 704, 1349
- Parrish I. J., Quataert E., Sharma P., 2009, ApJ, 703, 96
- Quataert E., 2008, ApJ, 673, 758